



Universiteit
Leiden
The Netherlands

Novel immune cell-based therapies for atherosclerosis

Frodermann, V.

Citation

Frodermann, V. (2015, May 27). *Novel immune cell-based therapies for atherosclerosis*. Retrieved from <https://hdl.handle.net/1887/33064>

Version: Corrected Publisher's Version

License: [Licence agreement concerning inclusion of doctoral thesis in the Institutional Repository of the University of Leiden](#)

Downloaded from: <https://hdl.handle.net/1887/33064>

Note: To cite this publication please use the final published version (if applicable).

Cover Page



Universiteit Leiden



The handle <http://hdl.handle.net/1887/33064> holds various files of this Leiden University dissertation

Author: Frodermann, Vanessa

Title: Novel immune cell-based therapies for atherosclerosis

Issue Date: 2015-05-27

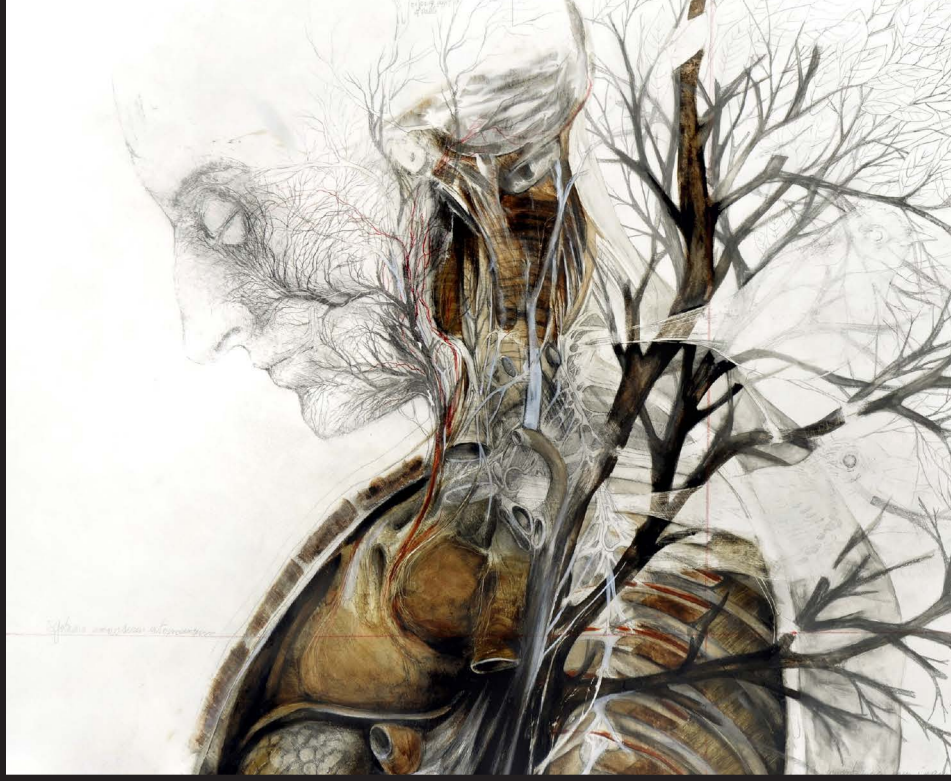
Vanessa Frodermann¹
Janine van Duijn¹
Melissa van Pel²
Peter J. van Santbrink¹
Ilze Bot¹
Johan Kuiper¹
Saskia C.A. de Jager^{1,6}

4

¹ Division of Biopharmaceutics, LACDR, Leiden University, Leiden, The Netherlands

² Department of Immunohematology & Blood Transfusion, Leiden University Medical Center, Leiden, The Netherlands

³ Present address: Laboratory of Experimental Cardiology, University Medical Center Utrecht, Utrecht, The Netherlands



Mesenchymal Stem Cells Reduce Murine Atherosclerosis Development

Submitted.



Abstract

Objective Mesenchymal stem cells (MSCs) have regenerative properties, but have recently received increasing attention for their immunomodulatory capacities. As atherosclerosis is an immune-mediated disease, we investigated whether MSCs could beneficially affect atherosclerotic lesion development.

Methods and Results The immunomodulatory capacity of murine MSCs was first determined *in vitro*. In a co-culture of MSCs and dendritic cells, MSCs significantly reduced TNF- α and increased IL-10 production by dendritic cells in response to LPS. Moreover, MSCs dramatically inhibited CD4⁺ and CD8⁺ T cell responses in a co-culture with splenocytes or isolated CD4⁺ T cells by preventing the differentiation of naïve T cells.

Next, we adoptively transferred MSCs into atherosclerosis-prone low-density lipoprotein-receptor deficient mice, which were fed a Western-type diet for eight weeks and subsequently assessed their effect on atherosclerotic lesion development. MSC-treated mice initially had higher levels of Tregs, while in the long-term, overall numbers of differentiated T cells were reduced by MSC treatment. Moreover, MSC-treated mice displayed a significant reduction in circulating monocytes and serum CCL2 levels. Interestingly, serum cholesterol levels were significantly reduced, due to a decreased VLDL production in the liver. Most importantly, MSCs induced a significant 33% reduction in aortic root lesion size and a 56% reduction in lesional macrophage content.

Conclusion We show here for the first time that MSC treatment significantly reduces atherosclerotic lesion development in mice and this may initiate future studies to assess the therapeutic capacity of MSCs in atherosclerosis patients.

Introduction

Mesenchymal stem cells (MSCs), also called bone marrow stromal cells or mesenchymal stroma cells, are multipotent cells that can give rise to cells of the mesodermal lineage, including adipocytes, osteocytes and myocytes¹. They were first identified in the bone marrow, but can be isolated from other tissues such as umbilical cord, placenta and adipose tissue². After isolation, MSCs can be easily expanded without losing their multipotency which renders them an interesting tool for therapeutic strategies¹. MSCs were initially investigated for their ability to repair injured heart tissue after myocardial infarction^{3,4}. They can migrate to sites of tissue damage and inflammation, where they can extravasate, engraft the tissues and reduce scar formation⁴⁻⁸.

In recent years the immunomodulatory capacity of MSCs has been increasingly appreciated. Several studies have investigated the capacity of MSCs to modulate both adaptive and innate immune responses^{2,9-14}. For instance, MSCs have been shown to reduce monocyte responses after myocardial infarction¹⁰ and to skew macrophages to an anti-inflammatory IL-10-producing phenotype¹⁰⁻¹³. MSCs also inhibit the differentiation and maturation of dendritic cells (DCs)¹⁴, by reducing the expression of co-stimulatory molecules and pro-inflammatory cytokines (TNF- α and IL-12), while increasing the production of anti-inflammatory cytokines (TGF- β and IL-10)^{15,16}, which indirectly suppresses T cell proliferation¹⁶. However, MSCs can also directly inhibit T cell proliferation¹⁵⁻¹⁷, by inducing cell cycle arrest in all subsets, resulting in a quiescent state and decreased proliferation¹⁸.

Inflammatory processes play a crucial role in all stages of atherosclerosis. Early in the disease process, entrapped oxidized low-density lipoprotein (oxLDL) leads to the activation of arterial endothelial cells and an ensuing recruitment of monocytes and T cells¹⁹. Upon recruitment, monocytes can differentiate to macrophages²⁰. Macrophages can primarily promote T cell responses to local antigens, while DCs can activate naïve T cells in response to lesion-derived antigens in draining lymph nodes²¹. DCs are also present within lesions or can arise from blood-derived precursors. Both macrophages and DCs express scavenger receptors, enabling the uptake of oxLDL and foam cell formation, and toll-like receptors, which mediate maturation of the antigen-presenting cells and production of pro-inflammatory cytokines. CD4⁺ T cells are crucially involved in the pathogenesis of atherosclerosis and their depletion results in a 70% reduction of lesion size²². The predominant subset in both human and murine atherosclerotic lesions is the Th1 subset^{23,24}, which produces a plethora of pro-inflammatory cytokines such as IFN- γ . IFN- γ promotes vascular inflammation by enhancing maturation and activation of antigen-presenting cells, increasing macrophage lipid uptake, reducing collagen production by SMCs, and enhancing expression of endothelial adhesion molecules, which subsequently stimulates leukocyte recruitment to the lesions²⁵. The continuous recruitment of further leukocytes to atherosclerotic lesions results in a vicious self-maintaining progressive inflammatory cycle. Nonetheless, it has been shown that by altering the phenotype of macrophages and DCs, they can become atheroprotective^{21,26,27}. Moreover, regulatory T cells (Tregs) have been clearly established as anti-atherogenic²⁸. Tregs produce high amounts of

the anti-inflammatory cytokine IL-10 and inhibit ongoing inflammation.

Due to the key role of inflammatory processes in the initiation and progression of atherosclerosis, adoptive transfer of MSCs, which have the capacity to modulate and reduce inflammation, may be a therapeutic approach to treat atherosclerosis. Preclinical studies have already shown that adoptively transferred MSCs are capable of modulating immune responses and they can prevent allograft rejection^{17,29} and alleviate autoimmune diseases³⁰⁻³². Moreover, in a phase II clinical trial, it was found that MSCs can reduce graft-versus-host disease³³. We now investigated the capacity of murine MSCs to affect the inflammatory process of atherosclerosis and thereby atherosclerotic lesion development.

Materials and Methods

Animals

C57BL/6 and LDLR^{-/-} mice were originally obtained from the Jacksons Laboratory, kept under standard laboratory conditions, and administered food and water *ad libitum*. All animal work was approved by the Ethics Committee for Animal Experiments of Leiden University and conforms to Dutch government guidelines.

DC culture

For DC cultures, bone marrow cells were isolated from the tibias and femurs of C57BL/6 mice. The cells were cultured for ten days at 37°C and 5% CO₂ in 10 cm² petri dishes in IMDM supplemented with 10% FCS, 1% penicillin/streptomycin (all obtained from PAA), 1% glutamax (Thermo Fisher Scientific) and 20 μM β-mercaptoethanol (Sigma Aldrich) in the presence of 20 ng/mL granulocyte-macrophage colony-stimulating factor (Peprotech). DC purity was assessed by CD11c expression (flow cytometry) and routinely found to be above 95%.

MSC isolation, phenotyping and labelling

Bone marrow cells were obtained by flushing femurs with washing medium (RPMI supplemented with 2% FCS, penicillin, streptomycin and L-glutamine). Next the bone marrow cells were cultured in a 75 cm² flask containing αMEM (Life Technologies) supplemented with 10% FCS (Greiner Bio-One), 2% penicillin/streptomycin (Life Technologies) and 1% L-Glutamine (Life Technologies; MSC medium). Subsequently, plastic adherent MSCs were cultured to 95% confluency in a fully humidified atmosphere at 37°C and 5% CO₂, harvested using trypsin and further expanded until sufficient numbers were obtained.

The MSCs that were used throughout this study were of passage six to eight; for in vivo MSC treatment cells of passage eight were used. MSC were phenotyped using the following antibodies: TER119 (clone TER119), CD31 (clone MEC 13.3), CD45.2 (clone 104), CD90.2 (clone 53-2.1), CD29 (clone HMB1-1), Sca-1 (Clone D7), CD105 (clone MJ7/18), CD44 (clone IM7) and CD106 (clone 429). All antibodies were obtained from BD Biosciences.

For tracking experiments, MSCs were labelled with 10 μM Carboxyfluorescein

succinimidyl ester (CFSE) according to manufacturer's protocol (Thermo Fisher Scientific). Briefly, MSCs were resuspended in prewarmed PBS/0.1 % BSA at a concentration of 1×10^6 cells/mL and incubated with dye at 37°C for 10 minutes in the dark. Afterwards, the staining was quenched by adding ice-cold media and incubating for another 5 minutes on ice, followed by three subsequent washing steps to remove excess CFSE.

Co-cultures

For DC-MSc co-cultures, 1×10^6 DCs were plated in 2 cm² non-tissue culture treated petri dishes (Greiner Bio-One) with indicated ratios of MSCs for 24 hours in MSC medium. DCs were stimulated with 100 ng/mL LPS to determine cytokine responses.

For splenocytes-MSc co-cultures, single cell suspensions of spleens from LDLr^{-/-} mice were obtained by using a 70 µm cell strainer (VWR International). Red blood cells were lysed with erythrocyte lysis buffer (0.15 M NH₄Cl, 10 mM NaHCO₃, 0.1 mM EDTA, pH 7.2). 1×10^5 splenocytes were added per well with indicated amounts of MSCs. For T cell-MSc co-cultures, CD4⁺ T cells (>95% purity) were isolated from splenocytes by using the BD IMag™ mouse CD4 T lymphocyte enrichment set according to manufacturer's protocol (BD Biosciences). 1×10^5 T cells were added per well with indicated amounts of MSCs. Both splenocytes and T cell-MSc co-cultures were cultured in quintuplicates in 96-well round-bottom plates (Greiner Bio-One) in the presence or absence of αCD3/28 (2 µg/mL, eBioscience) for 72 hours in complete RPMI 1640, supplemented with 10% FCS, 100 U/ml penicillin/streptomycin, 2mM L-glutamine (all obtained from PAA) and 20 µm β-mercaptoethanol (Sigma Aldrich). Proliferation was measured by Ki-67 expression by flow cytometry or addition of ³H-thymidine (0.5µCi/well, Amersham Biosciences) for the last 16 hours of culture. The amount of ³H-thymidine incorporation was measured using a liquid scintillation analyzer (Tri-Carb 2900R) as the number of disintegrations per minute (dpm). T cell subsets were determined by flow cytometry.

For splenocytes and T cell cultures in the presence of MSC culture supernatant, MSC culture supernatant was added in different concentration of total medium added. MSC supernatant was filtered using a 0.2µm filter to remove residual cells before use.

Atherosclerosis

Atherosclerosis was induced in 16 weeks old male LDLr^{-/-} mice by feeding a Western-type diet (WTD) (0.25% cholesterol and 15% cocoa butter; Special Diet Services). Mice received 3 *i.v.* injections of PBS or 0.5×10^6 MSCs every other day prior to eight weeks WTD.

Flow Cytometry

Mice were sacrificed and subsequently, blood and spleen were harvested. White blood cells were obtained as described above. 3×10^5 cells per sample were stained with the appropriate FACS antibodies. The following antibodies were used: Ly-6G (clone 1A8; BD Biosciences), CD11b (clone M1/70), CD11c (clone N418), CD4 (clone RM4-5; BD Biosciences), CD8 (clone 53-6.7; BD Biosciences), FoxP3 (clone FJK-

16s), Gata-3 (clone TWAJ), Ki-67 (clone SolA15), MHCII (clone AF6-120.1), ROR γ t (clone AFKJS-9), and T-bet (clone eBio4B10). All antibodies were purchased from eBioscience, unless stated otherwise. For intracellular staining, cells were fixed and permeabilized according to the manufacturer's protocol (eBioscience). FACS analysis was performed on the FACS Canto II and data were analysed using FACS Diva software (BD Biosciences).

In Vivo Imaging Systems (IVIS)

For MSC tracking experiments, 1×10^6 MSCs were stained with CFSE and injected *i.v.* Ex vivo imaging was performed by placing either whole animals or organs in the IVIS Lumina Imaging System (Xenogen) at indicated time points and analyzing fluorescence based on the manufacturer's recommendations. Fluorescence intensity was quantified as photons/sec/cm² by Living Image software (Xenogen).

Histological analysis

To determine plaque size, 10 μ m cryosections of the aortic root were stained with Oil-Red-O and haematoxylin (Sigma Aldrich). Corresponding sections were stained for collagen fibers using the Masson's Trichrome staining (Sigma Aldrich) or immunohistochemically with an antibody against a macrophage-specific antigen (MOMA-2, polyclonal rat IgG2b, 1:1000, Serotec Ltd.). Goat anti-rat IgG alkaline phosphatase conjugate (dilution 1:100; Sigma Aldrich) was used as a secondary antibody and nitro blue tetrazolium and 5-bromo-4-chloro-3-indolyl phosphate as enzyme substrate. To determine the number of adventitial T cells, CD3 staining was performed using anti-mouse CD3 (clone SP7, 1:150, Thermo Scientific). BrightVision anti-rabbit-HRP was used as secondary antibody (Immunologic). The section with the largest lesion and four flanking sections were analyzed for lesion size and collagen content, two sections were analyzed for T cell content. All images were analyzed using the Leica DM-RE microscope and LeicaQwin software (Leica Imaging Systems). The percentage of collagen in the lesions was determined by dividing the collagen-positive area by the total lesion surface area.

Real-time PCR

mRNA was isolated from the liver using the guanidium isothiocyanate method and reverse transcribed (RevertAid Moloney murine leukemia virus reverse transcriptase). Quantitative gene expression analysis was performed on a 7500 Fast real-time PCR system (Applied Biosystems) using SYBR Green technology. The expression was determined relative to the average expression of three housekeeping genes: succinate dehydrogenase complex, Subunit A (SDHA), hypoxanthine phosphoribosyltransferase (HPRT), and 60S ribosomal protein L27 (Rpl27). The following primer pairs were used:

Scd1:	5'-TACTACAAGCCCCGGCCTCC-3'	and 5'-CAGCAGTACCAGGGCACCA-3'
SREBP-1c:	5'-TCTGAGGAGGAGGGCAGGTTCCA-3'	and 5'-GGAAGGCAGGGGGCAGATAGCA-3'
SREBP-2:	5'-TGAAGCTGGCCAATCAGAAAA-3'	and 5'-ACATCACTGTCCACCAGACTGC-3'
SDHA:	5'-TATATGGTGCAGAAGCTCGGAAGG-3'	and 5'-CCTGGATGGGCTTGAGTAATCA-3'
HPRT:	5'-TACAGCCCCAAAATGGTTAAGG-3'	and 5'-AGTCAAGGGCATATCCAACAAC-3'
Rpl27:	5'-CGCCAAGCGATCCAAGATCAAGTCC-3'	and 5'-AGCTGGGTCCCTGAACACATCCTTG-3'

Cytokines

IL-10, TNF- α , IFN- γ and CCL2 were determined by ELISA (BD Biosciences) according to manufacturer's protocol.

Serum cholesterol levels

During the experiment, mice were weighed and blood samples were obtained by tail vein bleeding. Serum concentrations of total cholesterol were determined by enzymatic colorimetric assays (Roche Diagnostics). Precipath (standardized serum; Roche Diagnostics) was used as internal standard. The distribution of cholesterol over the different lipoproteins in serum was determined by fractionation of 30 μ l of serum using a Superose 6 column (3.2 x 300 mm, Smart-System; Pharmacia). Total cholesterol content of the effluent was determined as described above.

Statistical analysis

Values are expressed as mean \pm SEM. Data of two groups were analysed with a two-tailed Student's T-test. Data of three or more samples were compared by one-way ANOVA and data of two groups with two variables were analyzed by two-way ANOVA, both followed by Bonferroni post-testing. Statistical analysis was performed using Prism (GraphPad). Probability values of $P < 0.05$ were considered significant.

Results

MSCs were generated from the bone marrow of male C57BL/6 mice and their phenotype was confirmed by flow cytometry analysis. All MSCs expressed Sca-1, CD29, CD44, CD105 and CD106, while CD45, CD31 and TER119 were not expressed (Figure 1).

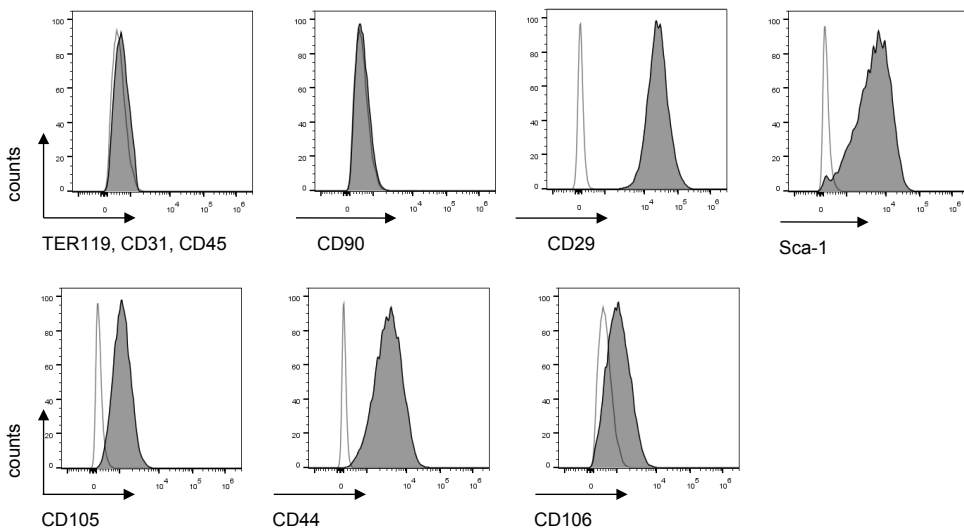


Figure 1. MSC Phenotype. MSCs were generated from the bone marrow of male C57BL/6 mice and the expression of surface markers was analyzed by flow cytometry. Representative histograms are shown.

To determine their immunomodulatory capacity, MSCs were co-cultured with DCs for three hours at different ratios, and subsequently stimulated with LPS. Twenty-four hours after LPS stimulation, we did not observe effects of MSCs on the expression of the co-stimulatory molecules CD40, OX40L and CD30L by DCs. The percentage of DCs positive for the co-stimulatory molecule CD86 increased by 12% and the percentage of DCs expressing the negative co-stimulatory molecule PD-L2 increased by 22%. The mean expression of CD86 per cell was however not significantly affected, whereas the mean expression of PD-L2 was decreased by 18% at higher MSC to DC ratios. The mean expression of the co-stimulatory molecule CD80 on DCs was significantly increased by 34% upon co-culture with MSCs (Table 1). CD80/CD86 function to induce T cell activation but can also promote Treg development, while PD-L2 functions to inhibit T cell activation, indicating that DCs might adopt a more tolerogenic phenotype after exposure to MSCs. In line with this, MSCs significantly affected the cytokine production of DCs in response to LPS. Pro-inflammatory TNF- α release was reduced by 57% while anti-inflammatory IL-10 production was increased by 45% (Figure 2A).

	DCs only	½ MSC per DC	1 MSC per DC	2 MSCs per DC	
CD80	95.5 ± 0.3	97.5 ± 0.4	98.2 ± 0.1	98.2 ± 0.1	Percentages
CD86	68.1 ± 0.7	73.8 ± 0.3 (***)	76.0 ± 0.1 (***)	76.5 ± 0.1 (***)	
CD40	88.9 ± 0.3	92.1 ± 2.0	90.1 ± 0.8	93.43 ± 0.2	
OX40L	35.5 ± 0.8	47.6 ± 3.7 (*)	43.2 ± 1.1	44.1 ± 0.4	
CD30L	18.2 ± 1.9	17.6 ± 1.2	19.5 ± 1.2	21.1 ± 1.5	
PD-L2	50.9 ± 0.6	56.5 ± 2.3	61.8 ± 0.9 (**)	62.5 ± 0.15 (**)	
CD80	12666 ± 118	15568 ± 407 (***)	16351 ± 321 (***)	16961 ± 272 (***)	
CD86	49906 ± 446	55290 ± 957 (***)	52075 ± 55	49102 ± 75	
CD40	12447 ± 177	12065 ± 1148	11825 ± 287	12622 ± 12	
OX40L	7439 ± 78	7655 ± 221	8196 ± 139	8135 ± 91	
CD30L	2943 ± 41	2953 ± 53	2924 ± 32	3018 ± 59	
PD-L2	5469 ± 105	5012 ± 100	4695 ± 211	4534 ± 76 (*)	

Table 1. MSCs only mildly affect co-stimulatory molecule expression of LPS-stimulated DCs. DCs were co-cultured with indicated ratios of MSCs for 3 hours prior to addition of 100 ng/mL LPS for 24 hours. DC numbers remained constant. Co-stimulatory molecules on DCs, determined as CD11c⁺MHCII⁺, were determined by flow cytometry. The percentage and mean fluorescence intensity (MFI) is shown. All values are expressed as mean±SEM and representative of two independent experiments done in triplicate. *** P<0.001

Since MSCs have been shown to affect T cell responses, we co-cultured MSCs with splenocytes from atherosclerosis-prone LDLR^{-/-} mouse in the presence of α CD3/CD28 for 72 hours. MSCs potently inhibited T cell proliferation by 99%, as measured by ³H-thymidine incorporation, compared to α CD3/CD28 stimulated splenocytes in the absence of MSCs. CD4⁺ T cell proliferation was reduced by 92% and CD8⁺ T cell proliferation by 87%, as measured by Ki-67 expression. Polarization of all CD4⁺ T cell subsets was inhibited to a similar extent (Th1 and Th2 more than 99% and Tregs by 89%; Figure 2B). Cytokine responses indicated similar effects: IL-10 production was not detectable, IFN- γ was reduced by 99%, and TNF- α showed a 92% reduction upon co-incubation with MSCs (Figure 2C). Co-cultures of isolated CD4⁺ T cells and MSCs

showed comparable, but milder effects: proliferation of T cells was on average reduced by 80%, the skewing towards specific T cell subsets was reduced by an average of 85% (Figure 2D and E). Interestingly, MSC culture supernatant had no effect on T cell proliferation, suggesting that cell-cell contact is crucial (data not shown).

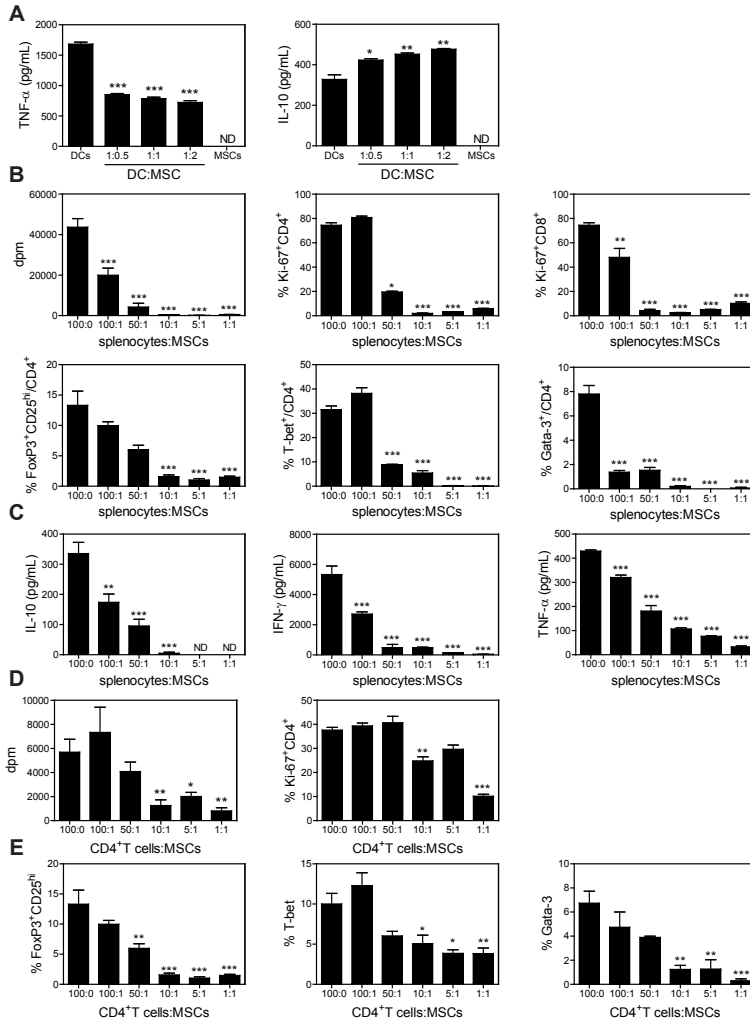


Figure 2. MSCs affect innate and adaptive immune responses. **A.** DCs were co-cultured with indicated ratios of MSCs for 3 hours prior to addition of 100 ng/mL LPS for 24 hours. DCs numbers remained constant. Cytokine responses were determined by ELISA. **B.** Splenocytes from an LDLR^{-/-} mouse were co-cultured with indicated ratios of MSCs in the presence of α CD3/CD28 for 72 hours. Proliferation was assessed by ³H-thymidine incorporation and Ki-67 expression by flow cytometry. Treg (FoxP3⁺CD25^{hi}), Th1 (T-bet⁺) and Th2 (Gata-3⁺) within CD4⁺ T cells were determined by flow cytometry. Splenocyte numbers remained constant. **C.** Cytokine responses by splenocytes were determined by ELISA. **D.** Proliferation of CD4⁺ T cells from an LDLR^{-/-} mouse in the presence of MSCs was assessed by ³H-thymidine incorporation and by Ki-67 expression by flow cytometry. CD4⁺ T cell numbers remained constant. Proliferation was assessed by ³H-thymidine incorporation and Ki-67 expression by flow cytometry. **E.** Treg (FoxP3⁺CD25^{hi}), Th1 (T-bet⁺) and Th2 (Gata-3⁺) within CD4⁺ T cells were determined by flow cytometry. All values are expressed as mean \pm SEM and representative of at least two independent experiments done in triplicate. *P<0.05, **P<0.01, ***P<0.001. ND defines not determined.

Before testing the effect of MSCs on atherosclerosis, we fluorescently labelled MSCs with CFSE (Figure 3A) and established the fate of fluorescently labelled MSCs after *i.v.* injection in *LDLR^{-/-}* mice on a cholesterol rich diet (WTD) and determined to which organs they migrated. MSCs initially accumulated primarily in the lungs and then slowly migrated out of the lungs (Figure 3B). One to three hours after injection, we found that MSCs had migrated to the liver, the heart, the draining lymph nodes of the heart and the aorta. Surprisingly, only few MSCs were recovered in the spleen (Figure 3C).

To test whether MSCs are able to modulate immune responses and thereby atherosclerosis, *LDLR^{-/-}* mice were treated with three *i.v.* injections of MSCs every

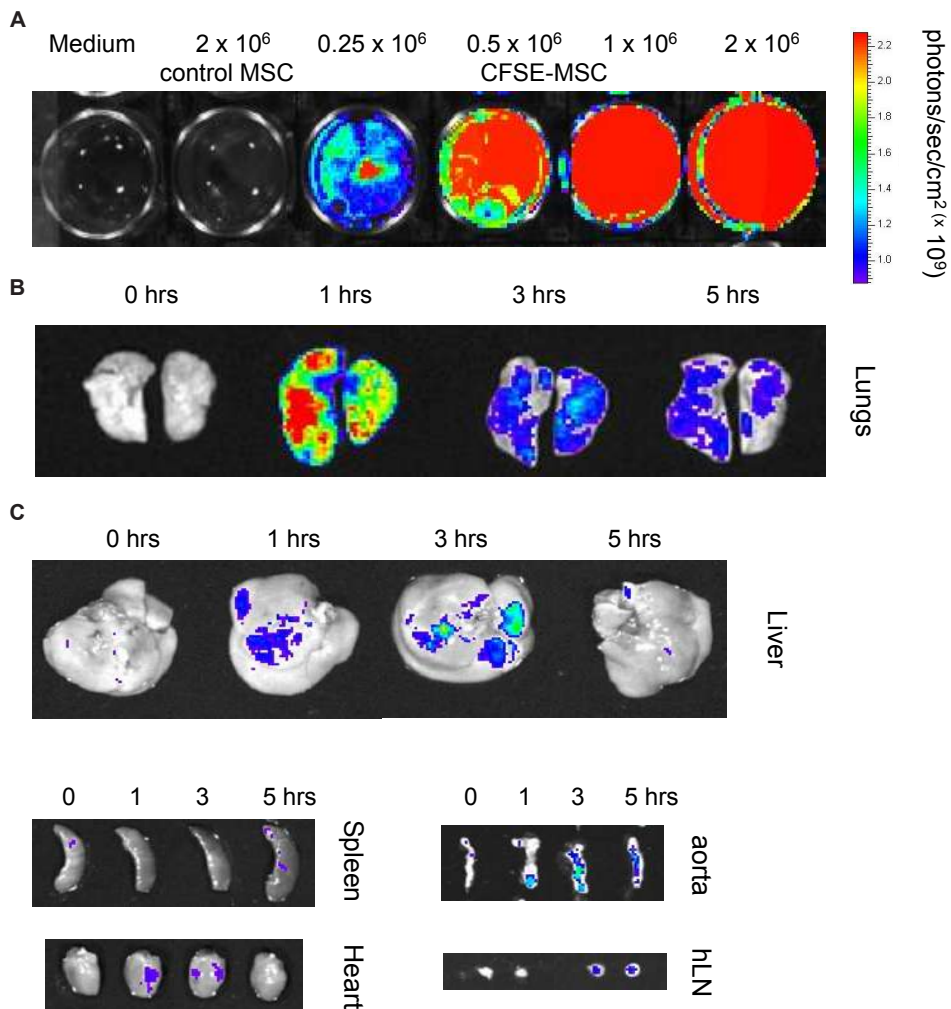


Figure 3. CFSE-labelled MSCs migrate preferentially to lung, liver, and the vasculature. A. MSCs were labelled with 10 μ M CFSE. Signal intensity on IVIS correlates with amount of cultured CFSE⁺ MSCs. Control MSCs indicates non-labelled MSCs. **B.** MSC presence in the lung 1-5 hrs after injections. **C.** Organ distribution of MSCs as determined by IVIS 1-5 hrs after injection of MSCs.

other day prior to induction of atherosclerosis by WTD feeding. One day after the start of WTD, we found a significant 38% drop in circulating CD4⁺ T cells (8.7% vs 14.1% for MSC vs control, respectively). Interestingly, we also observed an initial 51% increase in circulating Tregs (13.9% vs 9.2% for MSC vs control, respectively; Figure 4A). Eight weeks after inducing atherosclerosis, no difference in absolute white blood cell counts (data not shown) and percentage of circulating and splenic CD4⁺ T cells was found (Figure 4A and B). But a significant 18% decrease in splenic effector CD4⁺ T cells was still observed (Figure 4C). Both Th1 and to a lesser extent Tregs were significantly reduced in the circulation (44% and 10%, respectively), whereas this effect was not observed in the spleen. No significant effects of MSC therapy on Th2 cells were observed (Figure 4C).

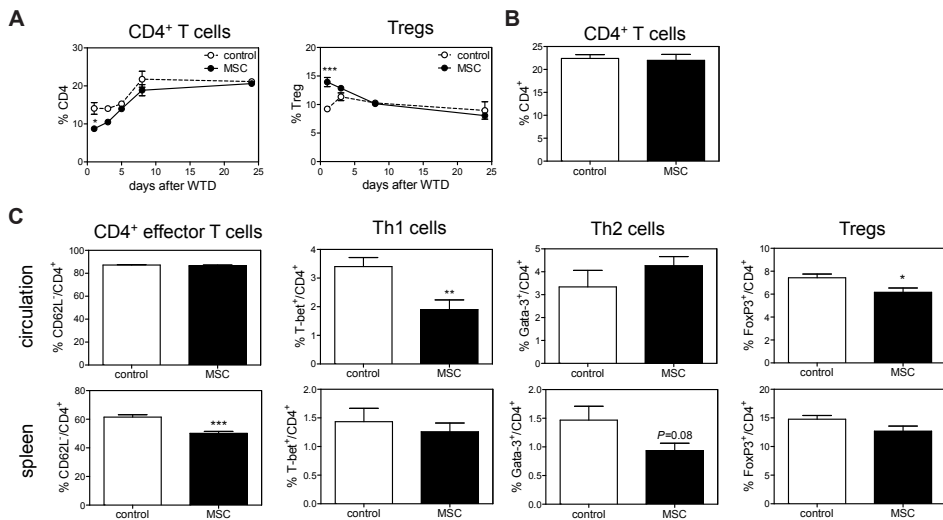


Figure 4. MSC-treatment affects CD4⁺ T cell responses in vivo. Male LDLr^{-/-} mice received three *i.v.* injections of either PBS (control) or 0.5 × 10⁶ MSCs (MSC) and were then fed a Western-type diet (WTD) for eight weeks. **A.** CD4⁺ T cells, as well as the percentage of FoxP3⁺ regulatory T cells (Treg) within CD4⁺ T cells, were measured in the circulation throughout the entire experiment by flow cytometry. **B.** After eight weeks, CD4⁺ T cells were determined in the spleen. **C.** After eight weeks, effector CD4⁺ T cells, determined as CD62L⁻ within CD4⁺ T cells, as well as T cell subsets of CD4⁺ T cells in the circulation and spleen were determined by flow cytometry. All values are expressed as mean ± SEM and representative of six mice. * P < 0.05, ** P < 0.01, *** P < 0.001.

Total CD8⁺ T cell numbers were not affected by MSC-treatment in the circulation throughout the entire experiment (Figure 5A) and were also not affected in the spleen after eight weeks of WTD (Figure 5B). However, we again found a 25% decrease in effector CD62L⁻/CD8⁺ T cells in the circulation and spleen after eight weeks WTD upon MSC-treatment (Figure 5C). To evaluate the proliferative capacity of T cells after MSC therapy, we isolated splenocytes eight weeks after induction of atherosclerosis by WTD feeding and cultured them in the presence of αCD3/CD28. In line with our *in vitro* data, splenocytes obtained from MSC-treated recipients showed a significant 30% decrease in T cell proliferation (Figure 5D). Furthermore, MSC treatment also significantly reduced circulating monocytes by 33%, which was directly associated

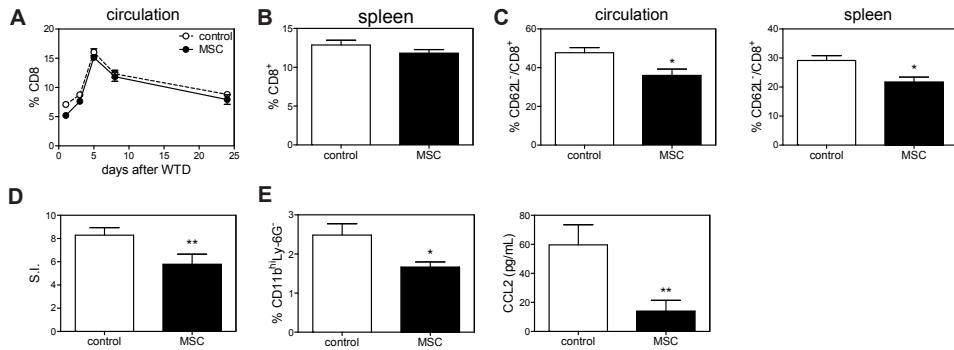


Figure 5. MSC-treatment affects CD8⁺ T cell and monocyte responses in vivo. **A.** CD8⁺ T cells were measured in the circulation throughout the entire experiment by flow cytometry. **B.** After eight weeks, splenic CD8⁺ T cells were determined by flow cytometry. **C.** Effector CD8⁺ T cells, determined as CD62L⁻ within CD8⁺ T cells, in the circulation and spleen were determined by flow cytometry. **D.** Splenocytes were isolated and stimulated with α CD3/CD28 for 72 hours. Proliferation was assessed by the amount of ³H-thymidine incorporation. Proliferation is normalized for proliferation of controls (without stimulation) and expressed as the stimulation index (S.I.). **E.** Circulating monocytes, determined as CD11b^{hi}Ly-6G⁻, were analyzed by flow cytometry. CCL2 levels in serum were determined by ELISA. All values are expressed as mean \pm SEM and representative of six mice. * P<0.05, ** P<0.01.

with a 77% reduction in serum CCL2 levels (Figure 5E), again suggesting a reduced inflammatory status of the MSC-treated mice.

Interestingly, we found a significant 33% reduction in serum cholesterol levels in MSC-treated mice after eight weeks WTD, but no effect on bodyweight (Figure 6A). The decrease in cholesterol levels was mainly a result of a decreased VLDL as assessed by FPLC analysis (Figure 6B). The effect on VLDL levels likely originated from reduced VLDL production, because liver mRNA expression of the rate-limiting enzyme

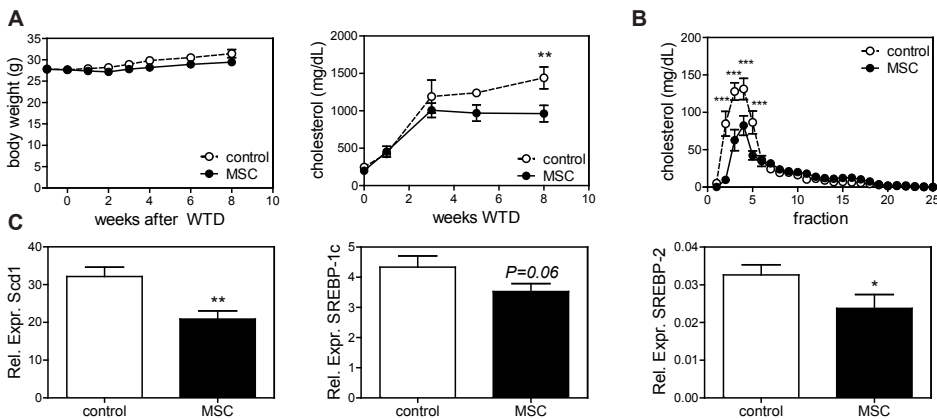


Figure 6. MSC treatment reduces VLDL production. **A.** Body weight and cholesterol levels were monitored throughout the entire experiment. **B.** Cholesterol distribution among plasma lipoprotein subclasses was determined by FPLC analysis after eight weeks WTD. For FPLC analysis serum of three mice was pooled. **C.** Liver mRNA expression of Scd1, SREBP-1c and SREBP-2 is shown, relative to the expression of three housekeeping genes (SDHA, HPRT and Rpl27). All values are expressed as mean \pm SEM and representative of all mice. *P<0.05, **P<0.01, ***P<0.001.

in fatty acid synthesis (Stearoyl-CoA desaturase-1, *Scd1*) was significantly reduced by 35%. Moreover transcription factors regulating fatty acid and cholesterol synthesis, sterol regulatory element-binding proteins 1c and 2 (SREBP-1c and SREBP-2) were reduced by 19% and 24%, respectively (Figure 6C).

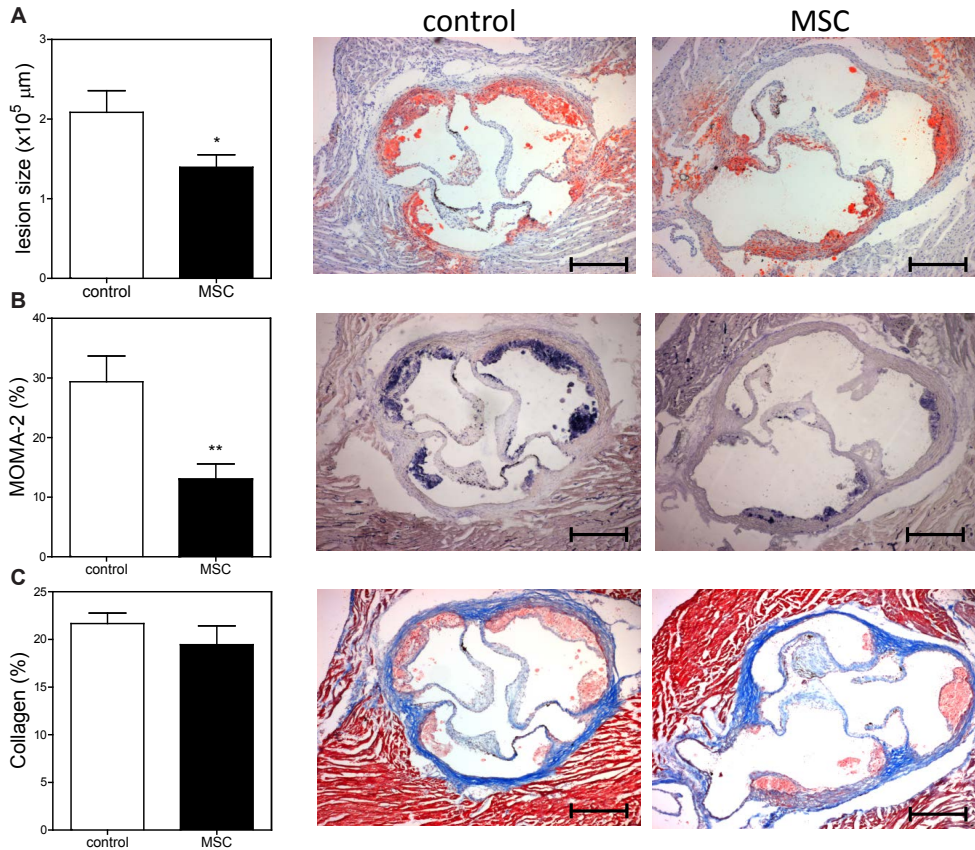


Figure 7. MSC treatment reduces lesion development. **A.** Lesion size in the three valve area of the aortic root was determined; representative cross-sections stained with Oil-Red-O and hematoxylin are shown. **B.** Macrophage content was determined by MOMA-2 staining as percentage of total lesion area. **C.** Collagen content was determined by Masson's Trichrome staining as percentage of total lesion area. Values are expressed as mean±SEM and representative of all mice. Scale bar, 300 μm. *P<0.05, **P<0.01.

The beneficial effects of MSC-treatment both on immune responses and cholesterol metabolism cumulated in a significant 33% decrease in atherosclerotic lesion size in MSC-treated mice ($1.4 \times 10^5 \pm 0.2 \times 10^5 \mu\text{m}$), compared with control mice ($2.1 \times 10^5 \pm 0.3 \times 10^5 \mu\text{m}$; Figure 7A). Additionally, we determined a significant 56% reduction in relative macrophage positive area of total lesion size (control: $29.4 \pm 4.3 \%$ vs. MSC: $13.0 \pm 2.6 \%$), indicating a reduced inflammatory status of the lesions (Figure 7B). Lesion stability was not affected as the collagen content, determined by Masson's trichrome staining, was not significantly different between the groups (control: $21.7 \pm 1.1 \%$ vs. MSC: $19.4 \pm 2.0 \%$; Figure 7C).

Discussion

Here we show that MSC treatment may be a promising strategy to reduce atherosclerotic lesion development. In agreement with previous studies^{1,15,17,18}, we describe that MSCs can reduce the production of pro-inflammatory cytokines by DCs and dramatically inhibit T cell proliferation. We further show that adoptive transfer of MSCs into LDLr^{-/-} mice results in an initial drop in circulating CD4⁺ T cell numbers. While this reduction was only observed initially after MSC transfer and induction of atherosclerosis by WTD feeding, a significant decrease in effector CD62L/CD4⁺ and CD62L/CD8⁺ T cells in the spleen was observed after eight weeks WTD, clearly indicating a reduced differentiation of naïve T cells, which is consistent with effects observed *in vitro*. In agreement, a significant decrease in circulating Th1 cells as well as Tregs was observed eight weeks after MSC transfer, although we did observe an initial increase in circulating Tregs. Since we observed an overall significant inhibition of T cell differentiation both *in vivo* and *in vitro*, we hypothesized that additional processes and cell types are needed for this initial increase in Tregs. It has been suggested that MSCs can induce apoptosis of T cells, which may explain the initial drop in CD4⁺ T cells observed *in vivo*, and that these apoptotic T cells are cleared by phagocytes, which in turn may induce Tregs³⁴. Therefore *in vivo* Tregs could initially be induced indirectly, while later the overall inhibition of T cell differentiation reduces Treg numbers. Additionally, MSC therapy significantly reduced circulating monocytes and serum CCL2 levels, again clearly suggesting reduced immune responses. This is in line with a previous study showing reduced monocytes after MSC therapy for myocardial infarction¹⁰. The reduced monocytes and their reduced recruitment to the lesions resulted in a significant 56% reduction in lesional macrophages.

Unexpectedly, we found significantly lower plasma cholesterol levels in MSC-treated mice, due to a reduction of VLDL levels, which is to our knowledge an effect that was not previously described upon MSC treatment. The effects of MSC therapy on plasma cholesterol levels only emerged around four to five weeks after treatment indicating that the effects of MSCs could be indirect, e.g. by modulation of other cell types. Previous studies have found a link between immune cells and cholesterol metabolism. For example lymphotoxins, which are expressed by CD4⁺ T cells and DCs, play a role in the homeostasis of these cells, but can also contribute to metabolic disease^{35,36}. CD4⁺ T cell expression of LIGHT, another ligand of the lymphotoxin receptor, increases plasma cholesterol levels, again showing a direct link between immune cells and cholesterol metabolism³⁵. Furthermore, an increased lifespan of DCs³⁷ and the adoptive transfer of mature DCs was found to correlate with decreased serum cholesterol levels³⁸. Hence a modulation of DCs by MSCs could also indirectly affect cholesterol metabolism. We hypothesize that the overall reduced inflammatory environment in MSC-treated mice, due to the immunomodulatory effects of MSCs on immune cells, affected VLDL synthesis, by downregulation of Scd1, SREBP-1c and SREBP-2. For example, TNF- α , which is downregulated upon MSC and splenocyte co-culture, has been shown to upregulate SREBP-1c³⁹, thereby increasing VLDL synthesis. Moreover, IL-10 overexpression has been shown to result in reduced plasma

cholesterol, mostly due to reduced VLDL, in LDLR^{-/-} mice⁴⁰.

Overall MSC therapy was highly effective in reducing both immune responses and improving dyslipidemia, the two driving forces behind atherosclerosis, and resulted in a significant 33% reduction in aortic root lesion sizes. Future studies will need to show the effect of MSCs on different stages of atherosclerosis, but our observations suggest that due to a combined effect on inflammation and plasma cholesterol levels a beneficial effect may be anticipated. For example, an increased stability of advanced lesions can be expected as IL-10 has been shown to promote lesion stability^{41,42}. The fact that we do not observe an effect on lesion stability is likely associated with early atherosclerotic lesions which contain a low amount of vascular smooth muscle cells. Recently, allogeneic MSCs were evaluated for their potential to repair ruptured lesions and were shown to increase regeneration of the inner endothelial lining and collagen fiber formation in the vessel wall⁴³, implying their potential for the treatment of progressed lesions. Moreover, it could for instance prove interesting to repeatedly administer MSCs to ensure a more effective treatment for long term intervention. Moreover a modulation of MSCs to enhance their anti-inflammatory capacities and/or their lifespan could prove interesting.

The drawback of some studies^{9,10} assessing the effect of MSCs on inflammation is that they employ human MSCs in SCID mice, which lack T and B cells. As these do not have a fully functional immune system it is difficult to examine the effect of MSCs on immune responses. Additionally, there have been reports that allogeneic MSCs can be rejected by recipient mice⁹. For these reasons, we performed an adoptive transfer of MHC-matched mouse MSCs into LDLR^{-/-} mice in our study to avoid host immune responses to the grafted MSCs and to be able to do the experiment in mice with a functional immune system.

To translate our findings to clinical application, we anticipate to replicate our studies using human MSCs in humanized mouse models for atherosclerosis, which can be humanized in their immune system, e.g. by transfer of human hematopoietic stem cells into SCID, NOG or NSG mice^{44,45}. Also, a more humanized cholesterol metabolism, such as in the ApoE*3/CETP-Leiden mice⁴⁶, would enable a confirmation of effects observed on VLDL metabolism. Taken together, our study provides first evidence that a MSC-based treatment strategy for atherosclerosis may be beneficial.

References

1. Pittenger, M. F. *et al.* Multilineage potential of adult human mesenchymal stem cells. *Science* 284, 143–7 (1999).
2. Bernardo, M. E. & Fibbe, W. E. Mesenchymal stromal cells: sensors and switchers of inflammation. *Cell Stem Cell* 13, 392–402 (2013).
3. Toma, C., Pittenger, M. F., Cahill, K. S., Byrne, B. J. & Kessler, P. D. Human mesenchymal stem cells differentiate to a cardiomyocyte phenotype in the adult murine heart. *Circulation* 105, 93–8 (2002).
4. Mangi, A. A. *et al.* Mesenchymal stem cells modified with Akt prevent remodeling and restore performance of infarcted hearts. *Nat. Med.* 9, 1195–201 (2003).
5. Barbash, I. M. *et al.* Systemic delivery of bone marrow-derived mesenchymal stem cells to the infarcted myocardium: feasibility, cell migration, and body distribution. *Circulation* 108, 863–8 (2003).
6. Amado, L. C. *et al.* Cardiac repair with intramyocardial injection of allogeneic mesenchymal stem

- cells after myocardial infarction. *Proc. Natl. Acad. Sci. U. S. A.* 102, 11474–9 (2005).
7. Silva, G. V *et al.* Mesenchymal stem cells differentiate into an endothelial phenotype, enhance vascular density, and improve heart function in a canine chronic ischemia model. *Circulation* 111, 150–6 (2005).
 8. Houtgraaf, J. H. *et al.* Intracoronary infusion of allogeneic mesenchymal precursor cells directly after experimental acute myocardial infarction reduces infarct size, abrogates adverse remodeling, and improves cardiac function. *Circ. Res.* 113, 153–66 (2013).
 9. Uccelli, A., Moretta, L. & Pistoia, V. Mesenchymal stem cells in health and disease. *Nat. Rev. Immunol.* 8, 726–36 (2008).
 10. Dayan, V. *et al.* Mesenchymal stromal cells mediate a switch to alternatively activated monocytes/macrophages after acute myocardial infarction. *Basic Res. Cardiol.* 106, 1299–310 (2011).
 11. Németh, K. *et al.* Bone marrow stromal cells attenuate sepsis via prostaglandin E(2)-dependent reprogramming of host macrophages to increase their interleukin-10 production. *Nat. Med.* 15, 42–9 (2009).
 12. Melief, S. M., Geutskens, S. B., Fibbe, W. E. & Roelofs, H. Multipotent stromal cells skew monocytes towards an anti-inflammatory interleukin-10-producing phenotype by production of interleukin-6. *Haematologica* 98, 888–95 (2013).
 13. Melief, S. M. *et al.* Multipotent stromal cells induce human regulatory T cells through a novel pathway involving skewing of monocytes toward anti-inflammatory macrophages. *Stem Cells* 31, 1980–91 (2013).
 14. Nauta, A. J., Kruisselbrink, A. B., Lurvink, E., Willemze, R. & Fibbe, W. E. Mesenchymal stem cells inhibit generation and function of both CD34⁺-derived and monocyte-derived dendritic cells. *J. Immunol.* 177, 2080–7 (2006).
 15. Aggarwal, S. & Pittenger, M. F. Human mesenchymal stem cells modulate allogeneic immune cell responses. *Blood* 105, 1815–22 (2005).
 16. Beyth, S. *et al.* Human mesenchymal stem cells alter antigen-presenting cell maturation and induce T-cell unresponsiveness. *Blood* 105, 2214–9 (2005).
 17. Bartholomew, A. *et al.* Mesenchymal stem cells suppress lymphocyte proliferation in vitro and prolong skin graft survival in vivo. *Exp. Hematol.* 30, 42–8 (2002).
 18. Glennie, S., Soeiro, I., Dyson, P. J., Lam, E. W.-F. & Dazzi, F. Bone marrow mesenchymal stem cells induce division arrest anergy of activated T cells. *Blood* 105, 2821–7 (2005).
 19. Hansson, G. K. Inflammation, atherosclerosis, and coronary artery disease. *N. Engl. J. Med.* 352, 1685–95 (2005).
 20. Weber, C., Zernecke, A. & Libby, P. The multifaceted contributions of leukocyte subsets to atherosclerosis: lessons from mouse models. *Nat. Rev. Immunol.* 8, 802–15 (2008).
 21. Taghavi-Moghadam, P. L., Butcher, M. J. & Galkina, E. V. The dynamic lives of macrophage and dendritic cell subsets in atherosclerosis. *Ann. N. Y. Acad. Sci.* 1319, 19–37 (2014).
 22. Emeson, E. E., Shen, M. L., Bell, C. G. & Qureshi, A. Inhibition of atherosclerosis in CD4 T-cell-ablated and nude (nu/nu) C57BL/6 hyperlipidemic mice. *Am. J. Pathol.* 149, 675–85 (1996).
 23. Frostegård, J. *et al.* Cytokine expression in advanced human atherosclerotic plaques: dominance of pro-inflammatory (Th1) and macrophage-stimulating cytokines. *Atherosclerosis* 145, 33–43 (1999).
 24. Zhou, X., Paulsson, G., Stemme, S. & Hansson, G. K. Hypercholesterolemia is associated with a T helper (Th) 1/Th2 switch of the autoimmune response in atherosclerotic apo E-knockout mice. *J. Clin. Invest.* 101, 1717–25 (1998).
 25. Voloshyna, I., Littlefield, M. J. & Reiss, A. B. Atherosclerosis and interferon- γ : new insights and therapeutic targets. *Trends Cardiovasc. Med.* 24, 45–51 (2014).
 26. Murray, P. J. & Wynn, T. A. Protective and pathogenic functions of macrophage subsets. *Nat. Rev. Immunol.* 11, 723–37 (2011).
 27. Chistiakov, D. A., Sobenin, I. A., Orekhov, A. N. & Bobryshev, Y. V. Dendritic cells in atherosclerotic inflammation: the complexity of functions and the peculiarities of pathophysiological effects. *Front. Physiol.* 5, 196 (2014).
 28. Foks, A. C., Lichtman, A. H. & Kuiper, J. Treating Atherosclerosis With Regulatory T Cells. *Arterioscler. Thromb. Vasc. Biol.* (2014). doi:10.1161/ATVBAHA.114.303568
 29. Reinders, M. E. J. *et al.* Autologous bone marrow-derived mesenchymal stromal cells for the treatment of allograft rejection after renal transplantation: results of a phase I study. *Stem Cells Transl. Med.* 2, 107–11 (2013).
 30. Zappia, E. *et al.* Mesenchymal stem cells ameliorate experimental autoimmune encephalomyelitis inducing T-cell anergy. *Blood* 106, 1755–61 (2005).
 31. Augello, A., Tasso, R., Negrini, S. M., Cancedda, R. & Pennesi, G. Cell therapy using allogeneic bone marrow mesenchymal stem cells prevents tissue damage in collagen-induced arthritis. *Arthritis Rheum.* 56, 1175–86 (2007).
 32. Fan, H. *et al.* Pre-treatment with IL-1 β enhances the efficacy of MSC transplantation in DSS-

- induced colitis. *Cell. Mol. Immunol.* 9, 473–81 (2012).
33. Le Blanc, K. *et al.* Mesenchymal stem cells for treatment of steroid-resistant, severe, acute graft-versus-host disease: a phase II study. *Lancet* 371, 1579–86 (2008).
 34. Akiyama, K. *et al.* Mesenchymal-stem-cell-induced immunoregulation involves FAS-ligand-/FAS-mediated T cell apoptosis. *Cell Stem Cell* 10, 544–55 (2012).
 35. Lo, J. C. *et al.* Lymphotoxin beta receptor-dependent control of lipid homeostasis. *Science* 316, 285–8 (2007).
 36. Upadhyay, V. & Fu, Y.-X. Lymphotoxin signalling in immune homeostasis and the control of microorganisms. *Nat. Rev. Immunol.* 13, 270–9 (2013).
 37. Gautier, E. L. *et al.* Conventional dendritic cells at the crossroads between immunity and cholesterol homeostasis in atherosclerosis. *Circulation* 119, 2367–75 (2009).
 38. Habets, K. L. L. *et al.* Vaccination using oxidized low-density lipoprotein-pulsed dendritic cells reduces atherosclerosis in LDL receptor-deficient mice. *Cardiovasc. Res.* 85, 622–30 (2010).
 39. Ruan, H. *et al.* Profiling gene transcription in vivo reveals adipose tissue as an immediate target of tumor necrosis factor- α : implications for insulin resistance. *Diabetes* 51, 3176–88 (2002).
 40. Von Der Thüsen, J. H. *et al.* Attenuation of atherogenesis by systemic and local adenovirus-mediated gene transfer of interleukin-10 in LDLR^{-/-} mice. *FASEB J.* 15, 2730–2 (2001).
 41. Mallat, Z. *et al.* Protective role of interleukin-10 in atherosclerosis. *Circ. Res.* 85, e17–24 (1999).
 42. Potteaux, S. *et al.* Leukocyte-derived interleukin 10 is required for protection against atherosclerosis in low-density lipoprotein receptor knockout mice. *Arterioscler. Thromb. Vasc. Biol.* 24, 1474–8 (2004).
 43. Fang, S.-M. *et al.* Allogeneic bone marrow mesenchymal stem cells transplantation for stabilizing and repairing of atherosclerotic ruptured plaque. *Thromb. Res.* 131, e253–7 (2013).
 44. Ito, M. *et al.* NOD/SCID/ γ (c)(null) mouse: an excellent recipient mouse model for engraftment of human cells. *Blood* 100, 3175–82 (2002).
 45. Shultz, L. D. *et al.* Human lymphoid and myeloid cell development in NOD/LtSz-scid IL2R gamma null mice engrafted with mobilized human hemopoietic stem cells. *J. Immunol.* 174, 6477–89 (2005).
 46. Van den Maagdenberg, A. M. *et al.* Transgenic mice carrying the apolipoprotein E3-Leiden gene exhibit hyperlipoproteinemia. *J. Biol. Chem.* 268, 10540–5 (1993).